Description of HPM generation in atmospheric air using the laser and klystron terminology

Mladen M. Kekez

***Abstract*—It is suggested that the HPM generation in atmospheric air can be accounted by the concept developed in the design of CO_2 and the excimer lasers. With this approach some part of the energy from the high voltage source is deposited in the high-speed electrons of the corona/spark discharges located in the resonant cavity. The cavity containing 100% reflector / mirror and partially transparent reflector / mirror, is arranged in such a way that RF/microwaves can bounce back and forth through the gain (corona/spark discharge) medium. This electromagnetic (radiation) wave causes the space charge waves in the glow/spark channel plasma. This process enables the bunching of high-speed electrons in the retarding zones of the space charge waves and the transfer of the energy from the corona /spark discharge into the radiation wave.**

It is believed that the same concept holds in the operation of the klystron, where the electron beam is used to generate the microwaves in the resonant cavities. The experimental results are presented to support these ideas.

***Index Terms*—HPM generation, klystron, resonant cavity, spark channel discharges**

I. INTRODUCTION

The essential feature in the microwave devices is the structure made of conductive material named the resonant cavity. In klystron, the cavity is placed to surround an electron beam of oscillating intensity, so that the cavity can extract the power from the electron beam. The oscillating electric and magnetic fields associated with the electron beam enter the cavity via the so-called cavity gap. The transfer of energy from the cavity to a waveguide/ coaxial cable is made via a coupling loop.

In 1939 the Varian brothers added a second cavity resonator so that the system has an input cavity and an output cavity. This input cavity (which is driven externally) is used to enable an electron beam of oscillating intensity i.e., to "bunch" and release packets of electrons, so they can be sent down the drift space between two cavities in a straight path by an axial magnetic field. The second cavity extracts energy/power from the electron beam. The Varian brothers called their invention the Klystron.

Examples of cavities used in modern high power klystrons are given by Benford *et al*. [1]. A low-impedance klystron has the cavities of long length, L and small heights. This configuration is known as the pillbox cavity. For these conditions Benford *et al*. [1] presented Eq. 1 stating that the length of the cavity can be related to the wavelength, λ of the signal to be amplified i.e. the cavity will resonate at the frequency of the designer's choice.

$$L \approx (2n+1)\,\lambda/4 \qquad n=\text{integral number} = 0, 1, 2,\ldots \qquad (1)$$

II. RESONANT CAVITY

The cavity is well defined in the experimental set-up shown in Fig. 2. Later, this information is used as the guideline to obtain the resonant cavity for the experimental work conducted in the arrangement given in Fig. 1. The cylinder, 8 is present in Fig. 1.

In the arrangement of Fig. 1 the multi spark channels were formed. In the arrangement shown in Fig. 2 the single spark channel was observed. Fig. 2 is the approximation of the test geometry used in the study of the HPM signal arising from the spark breakdown at the bushing of the mini-Marx generator. See Ref. [2].

To obtain Fig. 2 from Fig. 1, it was necessary to remove the cylinder, 8 and the "hot" plate, 2. The inner diameter of the "cold" plate was increased in such a way to enable a single spark channel to be created in 2 mm gap. The partial reflector was used in Fig. 1. In Fig. 2, the E-field probe of 5 to 10 cm in diameter was employed to perform the functions of being the partial reflector and the measuring device.

When the electrical field probe was placed 1 to 2 m away from the single spark discharge shown in Fig. 2, the waveforms containing the frequencies up to 16 GHz (=bandwidth of the oscilloscope) were recorded. For the given distance, it was observed that the experimental data were reproducible.

Moving the probe a few cm away from the previous position, different results were obtained. This suggests that the radiation waves at various frequencies are interacting (or interfering with one another) and the electric fields are changing accordingly.

To understand better the cause of interference and to avoid unwanted interaction between the radiation and the surrounding structures in the laboratory, detailed experiments

Manuscript received September 19, 2011; accepted February 22, 2012

M. M. Kekez is with High-Energy Frequency Tesla Inc., (HEFTI), 2104 Alta Vista Drive. Ottawa, Canada, K1H 7L8, (e-mail: mkekez@magma.ca, web: www.hefti.ca)

were conducted in the anechoic chamber. It was found that at certain distance, the electric probe records the radiation at a single frequency suggesting that the resonator is obtained. In this case, the round trip distance, 2d is equal to the integral number of wavelengths λ of the wave in this spatial resonator:

$$d = n \lambda / 2, \qquad n = \text{integral number} = 1, 2, 3... \qquad (2)$$

Here, d is the distance between the E-field probe and the "cold" copper ring, 3 shown in Fig. 2. Eq. 2 can also help us to understand some experimental data shown in the Appendix.

In the experiments done with the set-up of Fig. 2, the frequency of the resonator, f (=c/λ) must be set to match certain strong frequency line coming from the runaway high-speed electrons of the corona/spark discharge. The energy spectra curves of the runaway electrons of the corona discharge have been measured by Tarasenko *et al* [3] and found to be in the range of 50 to 400 keV. Tarasenko *et al* found that the runaway electrons are having several distinctive peaks at different energy levels. This suggests that, tuning of the resonant cavity in the experiments means searching for one of these peaks to get the maximum HPM from the system. In Ref. [2] the cavity was tuned at the frequencies of 1.575 GHz, 1.61 GHz and 2.35 GHz for brass cathode and copper anode. In Refs. [4,5] the best results at single frequency were obtained when the resonant cavity was tuned at frequencies of 1.69 GHz and 1.96 GHz for tungsten cathode and copper anode.

The probe must be held in parallel position in respect to the copper plate, 3. When the probe is held in horizontal position by the dielectric material, 6 of Figs. 1 and 2, the reflection of the electromagnetic wave by the plexiglass could be comparable to the reflection of the E-field probe. The probe and the plexiglass are assuming the role of partial reflector and the electromagnetic (radiation) wave is being reflected by the partially reflector in this quasi–optical cavity.

For most common type of optical glass, the index of reflection is about 1.52 and the reflectance of 4% for optical wavelengths. For plexiglass the index is 1.488 and for quartz 1.455. In the field of microwaves, the reflectance is a function of both frequency and the size of the object.

III SPARK CHANNEL DISCHARGES

In this study, 9-stage Marx generator having sub-nanosecond rise-time and low internal impedance was used. Some characteristics of the generator are given on the web: http://www.hefti.ca/. The charging voltage per stage was 17.5 kV. The separation between the inner diameter of the copper ring, 3 and the outer diameter of the plate, 2 of Fig.1 varied between 1.5 mm and 3 mm. When the voltage impulse reaches the electrode 1 and the plate 2, the voltage impulse sees an open-circuit enabling the voltage to double its value for a very short period of time. The electric field in this gap is highly non-uniformed and is in high MV/cm range.

The textbook by Meek and Craggs, [6] states that the formation of the spark channel is a complex phenomenon. The glow-like discharge is usually the first stage of the spark breakdown prior to the spark channel formation. During these processes the electron density in the center of the channel may reach 10^{17} cm $^{-3}$ range, then the density will fall due to the thermodynamic expansion of the channel and the shock waves are created. The ions and neutral particles are being pushed out of the center of the channel and the remaining conditions for the electrons in the center of the channel resemble that of the electron beam flow under "poor vacuum" condition.

The high-speed electrons in the spark channel are present and they can be the source for the generation of the microwaves with the aid of the cavity. The overall behaviour of high-speed electrons in the resonant cavity is analogous to the one taking place in the Klystron geometry.

IV THEORY

The common description of the Klystron operation is that the resonant cavity excites the space charge wave. In the first cavity of the Klystron, the fields are modulating the axial drift velocity of the beam electrons and are exciting the space charge wave growth on the beam. The interaction producing microwaves corresponds to the space charge interactions. However, these interactions are not fully described in the literature.

The proposed lasers–like concept of RF/HPM generation /amplification/super-radiance by Kekez [4,5 and 7] uses the theory of Liu and Tripathi [8] to describe the interaction of electromagnetic waves with the electron beams and plasma to generate the microwave radiation. It is believed that these processes hold for both, the klystron operating in vacuum and the laser-like concept of RF/HPM generation operating in atmospheric air.

It should also be noted that, the walls of the klystron cavity located at long distance away from one another could also be viewed as the mirrors of the quasi-optical cavity in the cross-sectional area, where the coupling loop is present. From this point of view, the electron beam is placed in the centre of the klystron cavity.

Kekez [4] has suggested that, the origin of the RF/HPM generation is due to the interaction of the electromagnetic wave with runaway electrons of the corona and spark channel plasma present at the border of the cavity or inside the cavity. This interaction enables the electromagnetic (radiation) wave of frequency, ω to cause the space charge waves in the corona and spark channel plasma.

Liu and Tripathi [8] have presented the case where the electrons are distributed uniformly along the x-axis where the x-component of the electron velocity is $\Delta = v_x - \omega/k$ (when viewed in the frame moving with the phase velocity of the wave, ω/k). Here, k is the wave number. Liu and Tripathi divide the electrons into two groups (A) $\Delta > 0$ and (B) $\Delta < 0$. Group A electrons (with the velocity, $v_x > \omega/k$) are accelerated in the accelerating zones of the space charge waves and retarded in the decelerating zones to spend more time there. In the retarding zones there is bunching of A group electrons and the transfer of the energy from the high-speed electrons in the glow discharge into the incoming wave. The slower moving electrons ($v_x < \omega/k$) of group B tend to bunch in the accelerating zones, gaining the energy from the wave. The

relative population of electrons with ($v_x > \omega/k$) and ($v_x < \omega/k$), determines the slope of the particle velocity distribution function at $v_x = \omega/k$ and will decide the net damping (absorption of the wave/heating of plasma) or growth (amplification) of the electromagnetic (radiation) wave.

The gain (amplification) at microwave frequencies does not imply "population inversion" such as that occurring in most lasers. The gain medium (molecular, atomic, electronic) in which the population inversion takes place produces the radiation at specific frequencies only.

The interaction of electromagnetic waves with runaway high-speed electrons of the corona/ spark channel plasma and / or E-beams is the broadband effect. These interactions can lead to microwave generation at different frequencies, with the output frequency determined only by the dimensions of the resonator.

V EXPERIMENTAL ARRANGEMENT

The arrangement is shown in Fig. 1.

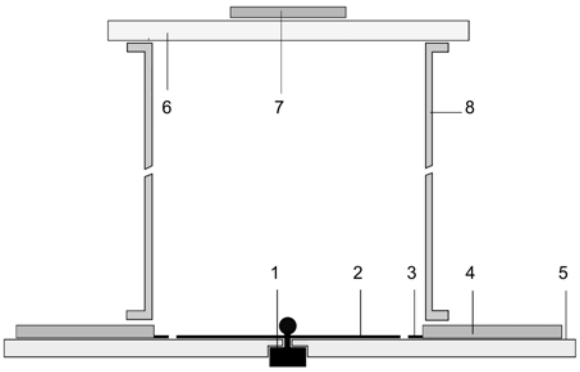

Fig. 1 shows the schematic of the experimental set-up.

1-HV output from the 9-stage Marx generator, 2 – "hot" copper plate 3 – "cold" copper ring, 4- ground flange of the generator, 5&6- plexiglass flange, 7-partial reflector, 8-cylinder. B-dot probe is placed above the partial reflector. Multi sparks channels are formed between the "hot" copper plate, 2 and "cold" copper ring, 3.

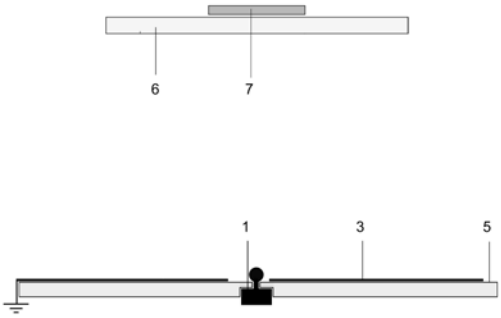

Fig. 2 shows the schematic of the experimental set-up.

Single spark channel is formed. The E-field probe is replacing the partial reflector of Fig. 1. The numbers are as in Fig. 1

When the Marx generator is triggered, the high voltage impulse reaches the copper disk, 2 and the corona/spark discharges occur between the "hot" electrode, 2 and the "cold" disk 3. The electrode structure is that of the circular rail spark gap characterized by the presence of the multi spark channels (with the characteristic number per length of the circumference). The electrode separation of the circular rail spark gap was kept constant (approximately 1.5 mm), while the diameters of the electrodes were varied. In the study few electrode pairs were used.

By increasing the diameter of the "hot" electrode, the number of spark channels is increased, hence the inductance minimized and the energy transfer enhanced from the Marx generator to the plasma in the channels. We are also observing the radiation output via the B-dot probe placed above the partial reflector.

The main point is to minimize the size of the cavity using the cylinder with straight walls, as shown in Fig. 1.

The radiation wave originating from each spark channel will be initially of semi-spherical shape until the wave hits the walls of the cylinder, 8. Interaction between the primary wave and the reflected waves takes place continuously. Certain fraction of the radiation wave is reflected by the partial reflector and the reflected wave traverse back towards the copper disk, 2.

If the inner surface of the cylinder, 8 would be of ellipsoidal shape, the tasks of ray-tracing method will be very much simplified. This is because the sum of the distances from any point on the ellipsoid to the two foci is constant and equal to the major diameter.

The idea of using an ellipsoid is not new. The drawing of the two-cavity klystron given in 2004 Encyclopedia Britannica Inc. shows that, the cavity is also (in part) of ellipsoidal shape. See: http://en.wikipedia.org/wiki/Klystron.

With the trial and error method and with various sets of electrodes, it was possible to get the radiation output at the single frequency with large energy content over long period of time.

The height of the cylinder was varied hoping to obtain the powerful signal in the range of 1.5 to 2 GHz with the copper cathode and copper anode. Eq. 2 has provided the guideline to obtain the appropriate height of the cylinder.

VI EXPERIMENTAL RESULTS

Fig. 3 shows the measured experimental data. To record the emissions over long period of time, the amplitudes of the emissions are partially clipped during the first 15 ns.

Fig. 4 is the experimental data obtained when the diameter of the "hot" electrode is decreased. The change of the frequency from 2.01 GHz observed in Fig. 3 to 1.75 GHz observed in Fig. 4, can be accounted in part by using Eq. 2. The effective length of the resonant cavity is increased in Fig. 4 stating that, the walls of the cylinder have dominant path in the propagation and the reflection of the waves.

The reproducibility of data can be improved considerably by designing 1.89 GHz helical antenna and positioning the antenna inside the cavity on the "hot" electrode.

The helical antenna was designed according to Ref. [9]. The helical antenna provides better coupling (i.e. kind of highway)

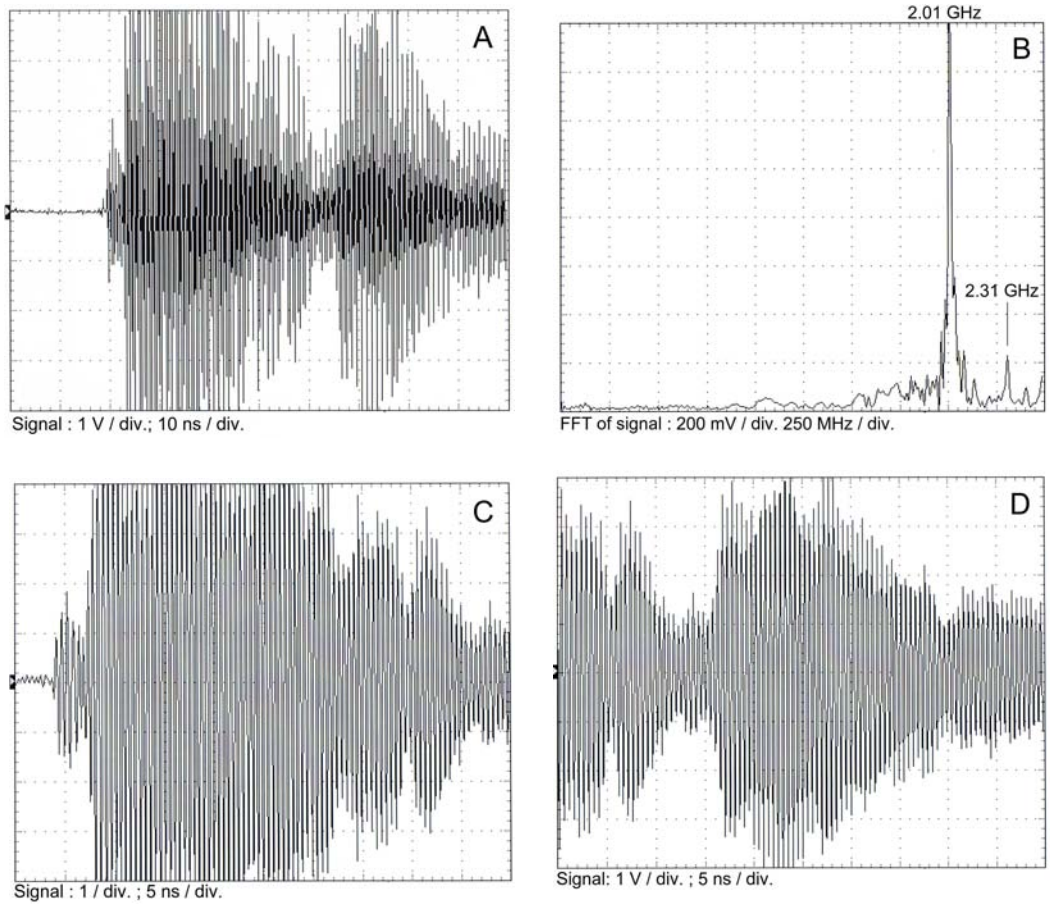

Fig. 3. Frame A is the signal and Frames B is FFT of the signal. Frames C and D show the signal of frame A on the faster time scale. B-dot probe is used. 9-stage Marx generator charged to 17.5 kV / stage is applied and the energy stored in the generator is 21 Joules

B-dot probe is calibrated in the TEM-cell. For frequency of 2.01 GHz, the amplitude of the signal of 1 Volt corresponds to the electric field of 1.62 kV/cm. The experimental set-up shown in Fig. 1 is used.

between 100% reflector and partial reflector and it is arranged in such a way that RF/microwaves can bounce back and forth through the gain medium. The antenna also suppresses the "chirping" processes, the well-known phenomenon observed in the vircator research. See Benford *et al*. [1]. However, there is still some variation in the shape and amplitude of the radiation pulse from shot to shot.

Using 30-stage Marx generator, it was demonstrated that, the reproducibility became very good when argon was used instead of atmospheric air. These experiments with argon were conducted at pressure of 500 to 600 Torrs.

Further advancement in the stability of the discharge was achieved by raising the voltage output in the Marx generator.

It should be stated that, the Marx generator must have a small internal impedance to facilitate the effective energy transfer, from the energy stored in the generator to the energy delivered to the plasma in the coronas and channels.

3 GHz oscilloscope was available for the current investigations. This oscilloscope has sufficient numbers of sample points to generate the correct amplitude of 1 GHz signal, when the signal is viewed with the time scale of 5 ns / div. When 10 ns / div. time scale is used, the envelope of the pulse is rather "rough" giving the appearance that the signal is subject to the "amplitude modulation". With 40 ns / div. scale, the oscilloscope cannot display correctly the signal at 1 GHz

To overcome some of these limitations in diagnostics, further work was conducted and three additional papers have been prepared.

In the first paper the measurements were performed to obtain additional details of the HPM generation in atmospheric air with the helical antenna. The second paper deals with the coherence processes of the HPM generation, which are responsible for the pulse shortening of the HPM pulse. The third paper gives the efficiency of HPM generation for the pulses of long duration.

VII DISCUSSION

The Marx generator is used to obtain the HPM generation in atmospheric air. When the same generator is used to drive the BWO system, it can be stated that, the BWO is far superior device in terms of power delivered to the target.

Not enough R&D data are available to make full comparison between the classical devices and the current approach in terms of energy conversion, reproducibility and reliability.

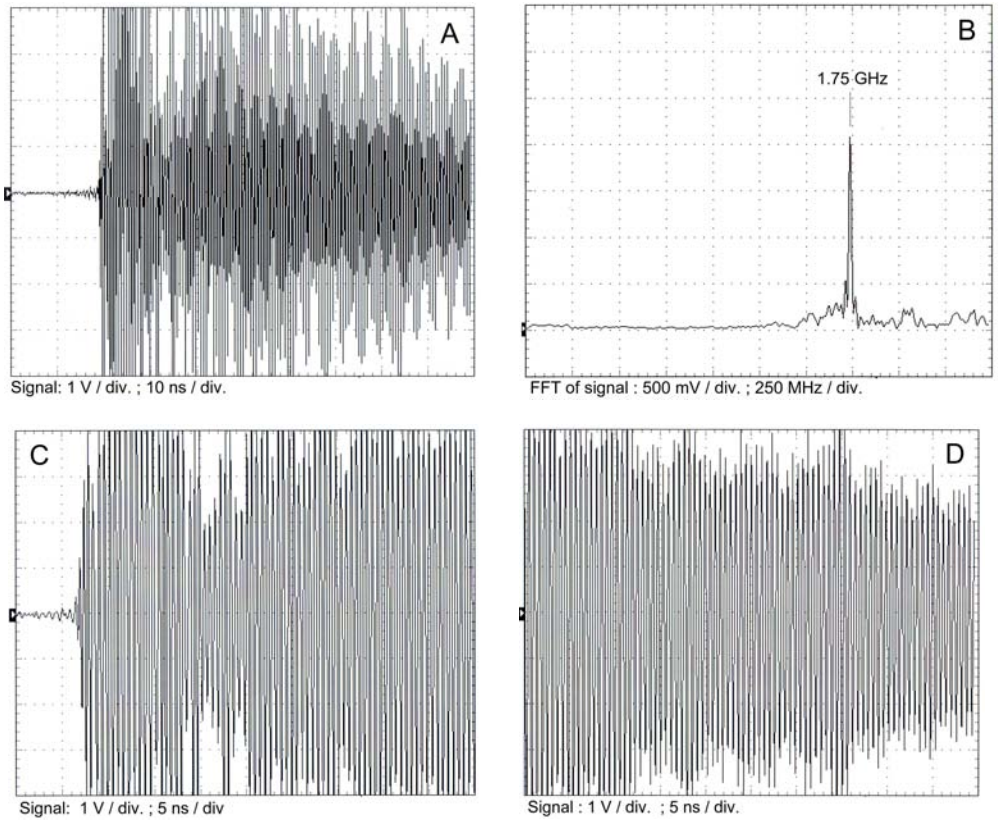

Fig. 4. Condition as in Fig. 2 except that the diameter of the "hot" electrode was decreased.

Frame A is the signal and Frames B is FFT of the signal. Frames C and D show the signal of frame A on the faster time scale

The theory presented needs further development to account for the experimental evidences. Here are two examples

Still photography shows that 4-8 spark channels of different brightness are formed between the "hot" copper plate, 2 and the "cold" copper ring, 3 in the experimental arrangement shown in Fig. 1. This suggests that the channels are not initiated or completed at the same time. The question now arises: what value the interacting electromagnetic wave must have to force the high-speed electrons in all the channels to release the radiation (energy) at the same frequency in a synchronized manner?

Further example of the experimental evidence is related to the tuning of the cavity. It was observed that, moving the same partial reflector on the plexiglass from the optimum position of 5 mm can cause the decrease of the signal amplitude by factor of 2 to 3. At optimum position the signal has maximum value.

It should be noted that in most cases whether the laser will work or not depends on the tuning of the mirrors (mainly the

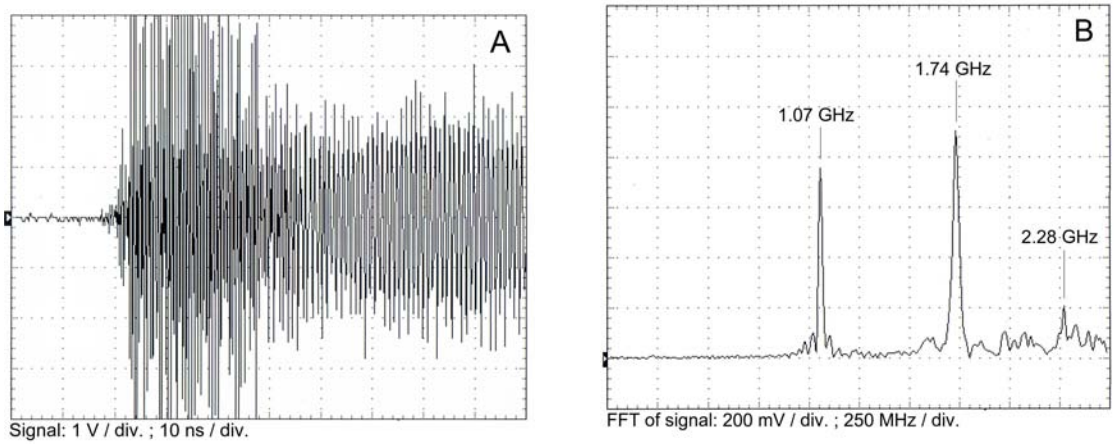

Fig. 5 shows the data with the "chirping" phenomenon. For the first 15 ns, the radiation is mainly at 1.74 GHz. Later the emission is at 1.07 GHz

HPM signal is given in Frame A and FFT of the signal is given in Frame B.

partial reflective mirror = output lens).

The simplicity of the design and low cost of doing R&D are the main attractive features of using the spark channels to generate the HPM emissions. This method can be used in conjunction with the explosively driven Magneto-Cumulative Generators (MCG), because the MCG have extraordinary large reservoir of energy.

For example, the output voltage up to 400 kV has been achieved by Sun *et al* [9] using electrically exploding switch in their small-size MCG capable of producing more than 20 GW into a 6 Ω resistive-load.

Chernyshev *et al* [11] have demonstrated that the increase of MCG power can be obtained by selecting the construction of foil opening switch having the extended break surface.

Using the condenser bank Chernyshev *et al* have achieved that the transfer of energy (with parameters: voltage, current and power) into the load were not lower than 420 kV, 10 MA, 2 10^{13} W respectively. Further work of Chernyshev's group has raised the high power voltage pulse to 1 MV with the pulse width of 300 ns.

The current experimental set-up could be just a minor add-on to the MCG to make the MCG a powerful HPM source.

REFERENCES

[1] J. Benford, J. A. Swegle and E. Schamiloglu, *High Power Microwaves*, Second editions, (NY; Taylor & Francis Group), 2007

[2] M. M. Kekez, "Understanding the HPM generation in atmospheric air with reference to small-size MCG", *the 17 IEEE Conf. on Pulsed Power, Washington, USA*, pp 1139-1146, June 28-July 2, 2009

[3] V. F. Tarasenko, E. H. Baksht, A. G. Burachenko, I.D. Kostyrya, K. I. Lomaev and D. V. Rybka, "Super-short avalanche electron beams in air and other gasses at high pressure" *IEEE Trans. Plasma Sci.*, **37**, pp. 832-839, 2009

[4] M. M. Kekez, "HPM generation in atmospheric air", *Proc. the 13 Int. Conf. on Megagauss magnetic field generation and related topics, Suzhou, China*, 2010 (also published on web: http://www.hefti.ca/)

[5] M. M. Kekez, "HPM amplification in atmospheric air", *Proc. the 13 Int. Conf. on Megagauss magnetic field generation and related topics, Suzhou, China*, 2010

[6] J. M. Meek J M and J. D. Craggs, *Electrical Breakdown of Gases*, John Wiley & Sons, Chicheter, UK, 1978

[7] M. M. Kekez, "RF/HPM super-radiance in atmospheric air, *Proc. the 13 Int. Conf. on Megagauss magnetic field generation and related topics, Suzhou, China*, 2010

[8] S. C Liu and V. K. Tripathi, "*Interaction of electromagnetic waves with electron beams and plasmas*", (Salem-World Scientific Publication Co. Pte. Ltd.), 1994

[9] J. D. Kraus and R. J. Marhefka, *Antenna for all applications*, Third Edition, McGraw Hill-Boston, 2002

[10] Q. Sun, C. Sun, X. Gong, W. Xie, S. Hao, Z. Liu, W. Dai, Y. Chi, W. Liu, M. Wang, N. Zhang and W. Han, "High power and high-voltage pulse generation on resistance loads by means of EEMGS" *Proc. 10th. Intl Conf. on Megagauss Field and Related Topics, Berlin, Germany*, pp. 201–206. July 2004

[11] V. K. Chernyshev, A.I Kucherov, A. B. Mezhevov, A. A. Petrukhin, and V. V. Vakhrushev "Electro-explosive foil 500 kV current opening switch characteristics research" *Proc. 11th IEEE Conf. on Pulsed Power, Baltimore, USA*, pp. 1208-1212, June 1987

[12] A. S. Marinčić, Nikola Tesla and wireless transmission of energy, *IEEE Trans. on Power Apparatus and Systems*, ***PAS 101****, pp 4064-4067, 1982*

[13] M. L. Burrows, *ELF communication antennas*, Stevenage Peter Peregrinus, 1978

[14] W. Jeon, J E. Lim, M. W Moon, K. B. Jung, W. B Oark, H. M. Shin, Y. Seo znd E.H. Choi. "Output characteristics of HPM generated form a coaxial Vircator with a bar reflector in a drift region". *IEEE Trans. on Plasma Science*, ***34,*** *pp 937-944, 2006*

[15] E. Schamiloglu, J. Gahl, C. Grabowski and C. Abdallah, "Approaches to achieving high efficiency, long pulse, vacuum BWO operation", *Beams'96, Prague, Czech Republic, June 10-14, 1996*

Biography: (not available)

APPENDIX

The appendix is presented in support of Eq. 2.

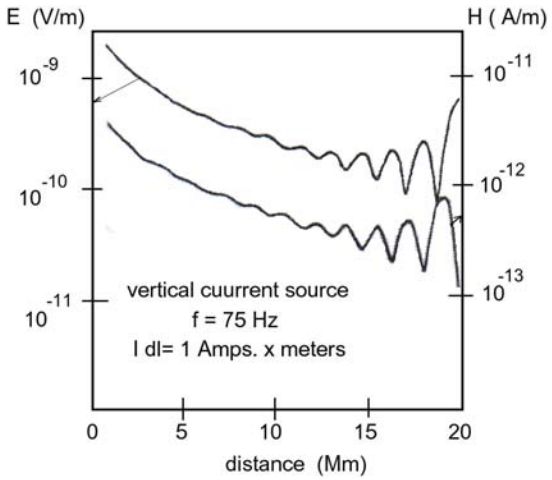

Fig. 1 shows the electromagnetic field in the earth-ionosphere waveguide. Refs. [12, 13]. Note 1 Mm=10^6 m. For 75 Hz, the wavelength, λ is 1.66 Mm. The peaks of E and H are pronounced between 15 and 20 Mm. The distance between the two adjacent peaks corresponds to λ and the product of E times H peaks at λ/2.

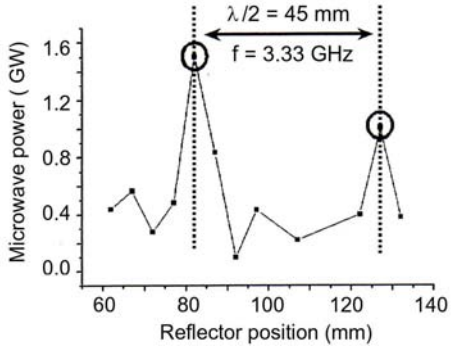

Fig. 2 shows the microwave power *vs.* reflector position for a coaxial Vircator with a bar reflector placed in a circular waveguide [14].

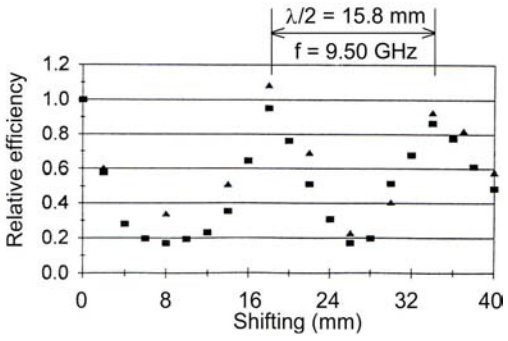

Fig. 3 shows the efficiency *vs.* shifting (= length of the circular waveguide added to the SWS in BWO system). Data points from Ref. [15].